Chemistry and Materials

The Center for Science Innovation

Research Article

Chem. Mater. 4 (3) 2025, 130-141

Synthesis of AuCu Bimetallic Nanoparticles via Electrodeposition for DPPH Free Radical Scavenging and HaCaT Cell Assays

Norma Nurul Ilmi[1]*, Putri Dwi Candra[1], Sabrina Putri Chaerani[2], Shirly Harissyah Alfiani[2]

[1]Department of Chemistry, Faculty of Mathematics and Natural Science, Universitas Negeri Jakarta, Jl. Rawamangun Muka, Jakarta 13220, Indonesia

[2]The Center for Science Innovation Arva Building, Jl. RP. Soeroso, Jakarta 10350, Indonesia

*Corresponding author: norma.nurulilmi0102@gmail.com

Received
19 July 2025

Received in revised form
18 September 2025

Accepted
22 September 2025

Published online
31 October 2025

DOI
https://doi.org/10.56425/cma.v4i3.113

Abstract

Bimetallic nanoparticles (NPs) have attracted significant interest in biomedical applications due to their unique physicochemical properties and synergistic effects. This study reports the synthesis of bimetallic gold-copper nanoparticles (AuCu NPs) via electrochemical deposition using cyclic voltammetry (CV) on indium tin oxide (ITO) substrates. Various precursor ratios of $HAuCl_4$ and $CuSO_4$ were employed to investigate the influence of Cu concentration on morphology and antioxidant activity of AuCu NPs. Characterization using field emission electron microscope equipped with energy dispersive X-ray spectrometer revealed that increasing Cu content altered the particle size distribution and surface uniformity, with optimal homogeneity achieved at a 1:1 Au:Cu ratio, yielding NPs of ~25–27 nm. X-ray diffraction analysis confirmed the presence of crystalline Au and Cu_2O phases, indicating successful co-deposition and surface oxidation of Cu. The antioxidant activity test, assessed through a DPPH radical scavenging assay, showed the highest inhibition (89.09%) for pure Au after a 48-hour incubation, whereas AuCu samples exhibited delayed yet substantial activity (>80%), suggesting time-dependent synergism. Furthermore, MTT assays on HaCaT cells revealed that the AuCu NPs were non-cytotoxic and exhibited protective effects against oxidative stress induced by blue light exposure, highlighting their potential for biomedical and dermatological applications.

Keywords: bimetallic AuCu, electrodeposition, antioxidant activity, DPPH assays

1. Introduction

Free radicals are unstable, reactive molecules that can damage proteins, lipids, and DNA, disrupting normal cell function [1]. An excess of free radicals causes oxidative stress, which is an imbalance between free radical production and the body's ability to remove them. This stress can contribute to chronic diseases like cancer, heart disease, diabetes, and Alzheimer's [2,3]. Persistent oxidative stress, if unchecked by antioxidants, causes cumulative tissue damage and accelerates cellular aging [4]. Consequently, scientists are increasingly focused on antioxidant compounds that can neutralize free radicals and boost the body's natural defences [5]. The primary role of antioxidants is to safely donate electrons to free radicals, stopping their destructive chain reaction and preventing damage to biological structures. [6].

Recent developments in the field of antioxidants have been closely linked to advances in nanotechnology, which allows for an increase in the active surface area of a material thereby increasing its capacity to counteract free radicals [7]. By reducing the particle size to the nanoscale, the chemical and physical properties of a material can change significantly, especially in terms of reactivity and absorption efficiency toward oxidative species [8]. In this context, various metal and metal oxide nanoparticles (NPs) such as ZnO, Cu_2O, Ni, and Co have been widely studied for their ability as potential antioxidant agents [9,10]. Among these materials, gold nanoparticles (AuNPs) have received

considerable attention due to their chemical stability, biocompatibility, and ability to reduce oxidative species through radical capture and electron transfer mechanisms [11]. Studies have also shown that the integration of metal NPs, such as Au and Cu, in bimetallic form is able to produce a synergistic effect that enhances antioxidant activity higher than the monometallic form [12]. Therefore, metal NPs, especially Au and Cu, are becoming the focus of innovative approaches to treat oxidative stress more effectively.

Gold NPs (AuNPs) have been reported to exhibit antioxidant activity by scavenging free radicals and modulating oxidative stress in biological systems [13]. In addition, AuNPs possess high biocompatibility, low cytotoxicity, and strong chemical stability, which support their safe application in biomedical research [14]. Their unique surface plasmon resonance (SPR) properties further enhance their reactivity in redox processes and contribute to light-driven antioxidant mechanisms. Several studies have also demonstrated high DPPH radical scavenging activity of AuNPs synthesized via green methods, including 85% inhibition using tangerine peel extract [15] and 70% inhibition with *Nerium oleander* leaf extract [16], confirming their effective role as antioxidant agents.

Copper (Cu) has antioxidant properties due to its role as a transition metal in redox reactions that can regulate the formation of reactive oxygen species (ROS). However, Cu can also trigger oxidative stress leading to programmed cell death such as cuproptosis [17]. In the study, CuNPs fixed on walnut shells (especially CuNP-WS3) showed significantly increased free radical scavenging ability of up to 94.82% at a concentration of 10 mg/mL, indicating high electron transfer potential [18]. A study by Laxmi Sonawane *et al.* (2021) also showed that green-synthesized CuNPs using *Dioscorea bulbifera* extract had a DPPH scavenging activity of 40.81 ± 1.44%, confirming their ability in redox reactions and electron stability in biological environments [19]. Meanwhile, Rajeshkumar *et al*. (2019) reported CuNPs synthesized using *Cissus arnotiana* extract showed antioxidant activity with a maximum DPPH free radical scavenging ability of 21% at a concentration of 40 µg/mL, which is close to the effectiveness of ascorbic acid (22%), indicating its potential as an active redox agent in biomedical applications [20].

Although AuNPs exhibit excellent biocompatibility, stability, and antioxidant activity [13,14], their relatively high cost and limited redox activity restrict broader applications. To address these limitations, Cu was selected as a complementary component because of its strong redox potential and affordability, despite its tendency to oxidize and its lower stability [20]. Conversely, compared to Cu and other transition metals, Au provides distinct advantages such as superior chemical stability, lower cytotoxicity, and unique plasmonic properties, which make it especially suitable for biomedical applications [13,14]. These features justify the selection of Au to be combined with Cu, as the combination is expected to balance high redox reactivity with stability and biocompatibility. The integration of Au with Cu is therefore considered a rational strategy to obtain synergistic properties, resulting in improved catalytic and antioxidant activity compared to their monometallic counterparts [13,20].

The effectiveness of AuCu bimetallic NPs has been widely studied because they provide higher antioxidant performance than their monometallic forms [21]. Elabbadi *et al.* (2023) reported that both core-shell structures and homogeneous AuCu alloys synthesized via electrodeposition methods produce particles with controlled morphology and good electrochemical stability, making them suitable for applications involving redox reactions [22]. In this system, Au stabilizes the surface and facilitates interactions with radical molecules, while Cu enhances the electron transfer rate through a reduction-oxidation mechanisms [23]. Research by Blosi *et al*. (2016) shows that AuCu NPs obtained through green methods exhibit stronger antioxidant activity and more uniform particle size distribution than monometallic NPs [24]. In addition, Razzaq *et al*., (2016) revealed that the presence of both metals can strengthen the antioxidant effectiveness of ascorbic acid in capturing free radicals due to increased interactions on the particle surface [25]. With these properties, AuCu bimetallic NPs have the potential to be used in various applications, such as protecting cells from oxidative stress, assisting tissue repair processes, and serving as active ingredients in nanotechnology-based products.

A wide variety of physical, chemical, and biological methodologies are used to synthesize AuNPs. Each of these methods has its own limitations such as high cost, potentially harmful effects, demanding labor requirements, and various other factors [26]. The electrodeposition method via cyclic voltammetry (CV) is a superior technique in the synthesis of AuNPs, as it produces particles with high purity while providing precise control over deposition conditions [27]. Parameters such as deposition potential range, number of voltammetry cycles, and scan rate greatly affect the size, density, and morphology of AuNPs formed, which in turn determine

their electron absorption ability and antioxidant activity [26].

The success of the electrodeposition process is determined not only by electrical parameters, but also by highly dependent on the selection of substrates that support charge transport and electrochemical stability. Indium Tin Oxide (ITO) is often chosen as a superior substrate for electrodeposition of bimetallic NPs such as AuCu due to its distinctive properties of providing high electrical conductivity (resistivity ~10^{-4} Ω-cm) and optical transparency >80% in the visible light range, allowing for in-situ electro-optical analysis as well as direct characterization of particle morphology [28]. In addition, the advantages of ITO are also seen in its resistance to electrochemical degradation during redox cycling, especially in the neutral to slightly acidic pH range [29]. A study by Zhang *et al*. (2015) also found that AuNPs synthesized through electrodeposition on ITO substrates adhered strongly and had a more uniform morphology than electrodeposition on other conductive glass substrates [30]. Therefore, this study aims to investigate the effect of varying $CuSO_4$ concentration on the morphology of AuNPs synthesized via CV-based electrodeposition method on an ITO substrate and to evaluate how these morphological changes influence the resulting antioxidant capacity.

2. Materials and Method

2.1 Materials

All materials used in this study were of analytical grade. The gold precursor was $HAuCl_4$-$3H_2O$ (Sigma-Aldrich) and the copper source was $CuSO_4$-$5H_2O$ (Merck). Potassium chloride (KCl) was used as a supporting electrolyte in the electrodeposition process. Indium Tin Oxide (ITO) coated glass was used as the substrate. Aquadest, aquabidest, technical-grade ethanol, analytical-grade ethanol, and aqua regia solution were used for the synthesis, dissolution, and cleaning processes.

2.2 ITO substrate preparation

The ITO substrates were first cleaned to remove organic and inorganic contaminants. The cleaning procedure involved sequential 15-minute ultrasonication baths in technical-grade ethanol and aquabidest then dried at room temperature.

2.3. Electrodeposition process of AuCu

AuCu nanoparticles (NPs) were synthesized via electrodeposition using cyclic voltammetry (CV). The electrolyte solution was prepared by dissolving $HAuCl_4 \cdot 3H_2O$ and $CuSO_4 \cdot 5H_2O$ precursors in 0.1 M KCl solution. The electrodeposition was carried out in a three-electrode electrochemical configuration, with ITO substrate as the working electrode, a platinum (Pt) foil as the counter electrode, and Ag/AgCl (3 M KCl) as the reference electrode. Synthesis was conducted at room temperature using CV at a potential window between -1.0 and +1.5 V, 50 cycles, and a scan rate of 125 mV/s. After the deposition process was completed, the film sample was rinsed by immersion in aquadest and ethanol. The compositional variations investigated in this study are listed in Table 1.

Table 1. Composition of electrolyte solution for the electro-deposition of AuCu NPs.

Sample	$[HAuCl_4]$ (mM)	$[CuSO_4 \cdot 5H_2O]$ (mM)	[KCl] (M)
Au-1	0.50	–	0.1
AuCu-2	0.35	0.15	0.1
AuCu-3	0.30	0.20	0.1
AuCu-4	0.25	0.25	0.1

2.4 Antioxidant activity test

The antioxidant activity of the synthesized AuCu NPs was evaluated using the 2,2-diphenyl-1-picrylhydrazyl (DPPH) radical scavenging assay. A 0.1 mM DPPH solution was prepared in methanol solvent, and the sample was dipped into the solution. Incubation was carried out at room temperature in the dark for two-time intervals, 30 minutes and 48 hours. The change in absorbance was measured using a UV-Vis spectrophotometer at a wavelength of 518 nm as an indicator of free radical scavenging activity. The radical scavenging efficiency was calculated as the percentage of inhibition using Equation (1):

$$\%Inhibition = \left(\frac{A_0 - A_1}{A_0}\right) \times 100\% \quad (1)$$

where A_o is the initial absorbance of DPPH solution, and A_1 is the absorbance of DPPH solution after reacting with the sample.

2.5. Characterization

The morphology and elemental composition of the samples was performed using a Field Emission Scanning Electron Microscope (FESEM, JEOL JSM-7600F) equipped with Energy Dispersive X-ray Spectroscopy (EDS, Oxford Instruments) to examine local elemental composition. The crystalline structure and phase identification were investigated using an X-ray Diffractometer (XRD, PANalytical X'Pert PRO, Co-Ka radiation (λ = 1.7903 Å) with a potential of 15 kV). The diffraction patterns were analyzed with HighScore Plus software using reference data from the Crystallography Open Database (COD) to

identify the crystal planes and the metallic phases formed in the samples.

2.6 MTT assay

The indirect cytotoxic and cytoprotective assays involving a pre-incubation of the samples for 72 hours as the initial stage to produce an immersion solution. Test samples were placed in a 48-well microplate containing 800 µL of medium, then incubated at 37°C and 5% CO_2. After 48 hours of incubation, HaCaT cells were implanted into a 96-well microplate and incubated for 24 hours. After cell attachment, the medium in the 96-well microplate was discarded and replaced with 100 µL of immersion solution from each sample with each sample tested in triplicate.

For the cytoprotective assay, the 96-well microplate was exposed to blue light for 6 hours, while for the cytotoxic assay no blue light exposure was done. After treatment, the media was discarded and the MTT assay was carried out by adding 10 µL of MTT solution, incubated for 3 hours. Subsequently, 100 µL of dimethyl sulfoxide (DMSO) was added and the plate was subjected to orbital shaking for 15 minutes. Absorbance was measured at a wavelength range of 400-600 nm. The percentage of cell viability was calculated based on the absorbance values.

3. Results and Discussion

3.1 Growth mechanism of AuCu NPs

The electrodeposition of AuCu NPs is generally described by a mechanism involving the stepwise reduction of metal precursors [31], as illustrated in Fig 1.

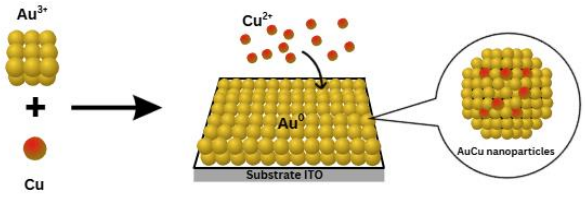

Figure 1. Illustration of the growth mechanism of AuCu nanoparticles [31].

The $AuCl_4^-$ ions are first reduced at a relatively positive potential, depositing Au^0 as initial nucleation sites. The deposited Au then acts as a nucleation center and an active site for the reduction of Cu^{2+} ions at a more negative potential. This stepwise process allows the controlled co-deposition of Au and Cu on the surface, forming a layer of bimetallic NPs with a homogeneous distribution. Such a mechanism is common in bimetallic electrodeposition, where the sequence of reduction potentials and surface interactions govern the final composition and structure of the alloy formed [21,23].

3.2 Morphological and elemental analysis

FESEM and EDS were used to analyze the morphology and elemental composition. Figure 2 shows that the AuNP-modified electrode surface has a dense, uniform morphology coated with fine particles that are relatively evenly distributed over the entire surface of the ITO substrate. Figure 2a reveals coarse-grained structures with small aggregates scattered across the surface, indicating the success of the electrodeposition process. The presence of fine cracks is most likely caused by surface tension during the particle growth process or during the drying stage. However, the AuNPs still formed a continuous and fused layer, reflecting the formation of a compact and active AuNPs film on the ITO substrate. EDS analysis shows that the elemental gold (Au) is distributed in the form of high-intensity local agglomerations, as shown in the Quant Map of Fig 2b, while carbon (C) and oxygen (O) are evenly distributed as possible residual organic matter, and silver (Ag) appears only minimally. This is reinforced by the Count Map in Fig 2c, which shows bright spots in the Au-concentrated area. Based on image analysis using ImageJ software, it was found that the average size of the deposited AuNPs was 31 nm. This size is within the optimal range widely reported in the literature as a major determinant of enhanced antioxidant activity, as the high surface-area-to-volume ratio allows for more efficient interaction with free radicals. The study by Dehghani *et al*. (2023) showed that green-synthesized AuNPs using *Glaucium flavum* extract had an average size of about 32 nm and exhibited significant antioxidant activity in DPPH assay, even at low concentrations [32]. Similar results were also reported by Tejaswini *et al*. (2023), where AuNPs of 20-30 nm obtained from *Capsicum annuum* extract showed a DPPH radical scavenging efficiency of 86% at a concentration of 100 µg/mL [33].

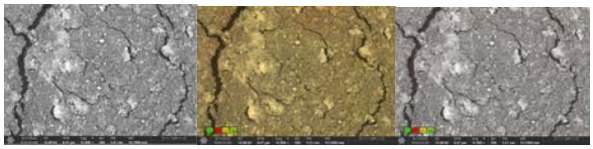

(a) **(b)** **(c)**

Figure 2. FESEM–EDS analysis of Au-1 nanoparticles.

In Fig 3a, the particles appear evenly distributed with relatively small and homogeneous size, indicating controlled growth. This morphology reflects the success of the AuCu co-deposition process, where AuNPs formed first act as nucleation centers for the continued growth of CuNPs, resulting in a structurally fused mixed-metal film. Elemental mapping via EDS Quant Map (Fig 3b) shows that the distribution of Au is localized to the main agglomeration area, while C and O are evenly distributed

across the surface. The Count Map (Fig 3c) supports this finding, showing high intensity in the metal agglomeration area, as well as low intensity and dispersed in other areas. Based on image processing using ImageJ, it was found that the average size of the NPs was 57 nm. The addition of Cu with a certain concentration is known to affect the size and structure of the formed NPs. In bimetallic systems such as AuCu, the presence of a second metal such as Cu plays a role in modifying the final particle morphology and can trigger the formation of core-shell structures or homogeneous alloys depending on the synthesis conditions. B. Akilandaeaswari *et al*. (2021) showed that the formation of AuCu NPs through a green synthesis approach resulted in morphologically stable particles and exhibited better biological activity than monometallic particles, which reinforces the notion that the bimetallic structure supports more optimized functional characters [34].

(a) **(b)** **(c)**

Figure 3. FESEM–EDS analysis of AuCu-2 nanoparticles.

Figure 4a shows a dense and highly uniform surface morphology, composed of fine spherical NPs with a very even distribution across the substrate surface. Elemental mapping analysis via EDS Quant Map (Fig 4b) shows intense and broad distributions for gold (Au) and copper (Cu) elements, which overlap in the nanoparticle area. The presence of Au and Cu signals at the same location supports the indication of co-deposition of both metals on the electrode surface. The Count Map (Fig 4c) reinforces this finding by showing bright spots in areas with high concentrations of Au and Cu with an average size of approximately 27 nm. This result reflects the synergistic effect of the co-deposition of Au and Cu metals during the electrodeposition process. The addition of Cu to the bimetallic system not only acts as a structural component but also affects the nucleation mechanism and particle growth. Higher concentrations of Cu can accelerate the initial nucleation process, thereby inhibit continued crystal growth and yielding particles with smaller sizes and more uniform distributions. This result is in line with the findings of Elabbadi *et al*. (2023), who reported that increasing the Cu ratio in the AuCu system improves morphological stability and inhibit particle overgrowth, resulting in nanocatalysts that are more size-controlled and evenly distributed on the substrate surface [22]. These findings indicate that the ~27 nm-sized AuCu structures formed in this study are the result from controlled co-deposition conditions, with significant contributions of Cu in improving dispersion and strengthening inter-particle attachment at the nanoscale.

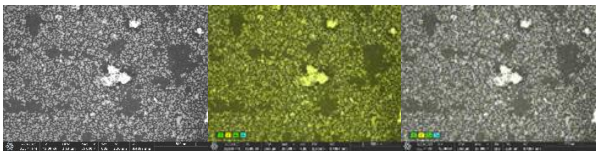

(a) **(b)** **(c)**

Figure 4. FESEM–EDS analysis of AuCu-3 nanoparticles.

Figure 5a shows a dense and highly uniform surface morphology, composed of fine spherical NPs with a very even distribution across the substrate surface. There are fewer large aggregates, indicating that particle growth is more homogeneous at a balanced Au:Cu ratio. Elemental mapping analysis via EDS Quant Map (Fig 5b) shows that gold (Au) is intensely and widely distributed, while carbon (C) and oxygen (O) are more homogeneously distributed across the surface, possibly from residual organic matter or interaction with the substrate surface. The Count Map (Fig 5c) reinforces these findings by showing bright spots in areas of high Au concentration with an average size of 25 nm. This result indicates the significant effect of adding Cu in a 1:1 ratio to the AuCu co-deposition process. When Cu is added in an amount equivalent to Au, it can accelerate the nucleation process and result in more controlled particle growth, so that the final particle size becomes smaller and the distribution is more even. This is in line with the results of a study by Blosi *et al*. (2016), who reported that AuCu NPs with an Au:Cu ratio of up to 1:1 produced a monodisperse size distribution of about 17-20 nm due to optimal equilibrium between the two metals [24]. The study reinforces the conclusion that a balanced Au:Cu ratio improves morphology control and prevents the formation of large aggregates.

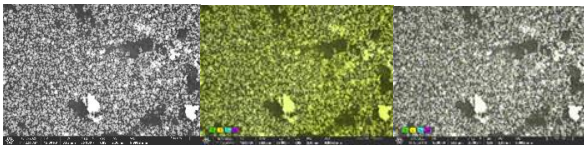

(a) **(b)** **(c)**

Figure 5. FESEM–EDS analysis of AuCu-4 nanoparticles.

Elemental mapping shown in Fig 6 illustrates the transition from pure Au deposition to the onset of bimetallic film formation upon Cu introduction. In the Au-1 sample, Au distribution is intense with no detectable Cu signal, consistent with pure AuNPs deposition. The high Au content (69.9 wt%) with dominant O and C background originates from the ITO substrate, confirming that the film is Au-dominated. In contrast, the AuCu-2 sample reveals

the first detectable Cu signal (0.3 wt%), accompanied by a decrease in Au content to 37.6 wt%. This indicates that co-deposition occurs, though surface segregation still favors Au dominance.

This trend agrees with the FESEM observations, where initial Cu addition produced larger, more aggregated particles. Cu appears to interfere with early nucleation events, leading to less controlled growth. Nevertheless, elemental mapping shows that Cu becomes more spatially dispersed compared to Au-1, suggesting the onset of a more homogeneous bimetallic structure. These results highlight that the Au:Cu precursor ratio not only dictates chemical composition but also influences nucleation dynamics and the overall uniformity of the deposited film. The dominance of Au on the surface, even with the addition of Cu in the AuCu-2 sample, is consistent with the concept of surface segregation, where the metal with lower surface energy (Au) tends to occupy the outer layer of the particle.

This observation aligns with the findings of Van Thuan *et al*. (2015), who reported that the formation of AuCu alloys is strongly influenced by reduction conditions, electrode potential, and the ion exchange rate at the interface [23]. Therefore, the elemental mapping results not only reflect the initial composition but also emphasize that electrodeposition conditions play a critical role in determining elemental distribution and the stability of the bimetallic phase.

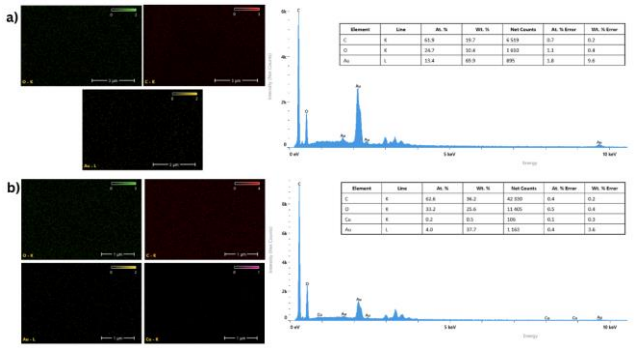

Figure 6. EDS elemental mapping of electrodeposited Au-1 (a) and AuCu-2 nanoparticles on ITO substrate (b).

Increasing the Cu concentration had a pronounced effect on the evolution of particle size and morphology (Table 2). The particle size increased in AuCu-2 (~57 nm), but decreased again in AuCu-3 and AuCu-4 (~25–27 nm) with a more uniform distribution. EDS analysis confirmed Au as the dominant element, while Cu was detected only in small amounts but became more homogeneously distributed at higher AuCu ratios. These findings highlight that balanced AuCu ratios promote more controlled NP growth.

Table 2. Summary of FESEM-EDS analysis of AuCu nanoparticles.

Sample	Average Particle Size (nm)	Morphology (FESEM)	Composition (EDS, main elements)
Au-1	~31 nm	Dense, uniform morphology, continuous AuNPs film	Au dominant (69.9 wt%), minor C, O, trace Ag
AuCu-2	~57 nm	Granular particles, local agglomerations, less controlled growth	Au 37.6 wt%, Cu 0.3 wt%, C and O background
AuCu-3	~27 nm	Spherical particles, highly uniform distribution	Au 32.0 wt%, Cu 0.6 wt%, more homogeneous distribution
AuCu-4	~25 nm	Highly uniform nanoparticles, homogeneous growth, minimal aggregates	Au dominant, Cu ~0.6 wt%, homogeneous overlap

3.3 Structural analysis

XRD analysis of the samples showed a typical pattern of gold (Au) face-centered cubic (fcc) crystal structure, with main diffraction peaks at about 44.6° and 55°, indexed as (111) and (200) planes, respectively, according to JCPDS reference data 01-089-3697. Additionally, diffraction peaks at around 38° and 64° correspond to the (111) and (220) planes of the fcc Au and Cu phases (JCPDS card No. 04-0784 for Au and No. 04-0836 for Cu). This supports the successful incorporation of both Au and Cu crystalline phases in the deposited films. In the control sample (sample Au-1) without Cu^{2+} addition, the XRD pattern displays sharp and intense Au (111) and Au (200) peaks, indicating a clean reduction of $HAuCl_4$ to crystalline Au^0 without any impurity phase. The addition of $CuSO_4$ in samples AuCu-2, AuCu-3 and AuCu-4 showed significant changes in the diffraction pattern. In sample AuCu-4, an additional peak appeared around 37°, which was identified as the (111) plane of Cu_2O (COD 00-002-1225).

The intensity of the Au peak decreased in proportion to the $HAuCl_4$ concentration in each sample. Sample Au-1 with 0.5 mM $HAuCl_4$ produced the sharpest and most intense Au (111) and Au (200) peaks, while in sample AuCu-4 with 0.25 mM $HAuCl_4$, the peak intensity significantly reduced. The same thing also happened to the Cu_2O peak.

The presence of the Cu_2O phase is attributed to the oxidation of the Cu^0 metal surface produced during deposition. In the co-reduction deposition process, Cu^{2+} ions are reduced to Cu^0 on the substrate surface along with the reduction of Au^{3+} to Au^0. After deposition, the more reactive Cu^0 metal is easily partially oxidized by dissolved oxygen or air into Cu_2O. This explains why the intensity of the Cu_2O peak increases at higher $CuSO_4$ ratios (sample AuCu-4), as more deposited Cu^0 is available for oxidation. In contrast, at higher Au:Cu ratios (sample AuCu-2 and AuCu-3), the intensity of the Au peak is stronger and the Cu_2O peak weakens or disappears due to the smaller amount of Cu^0 formed.

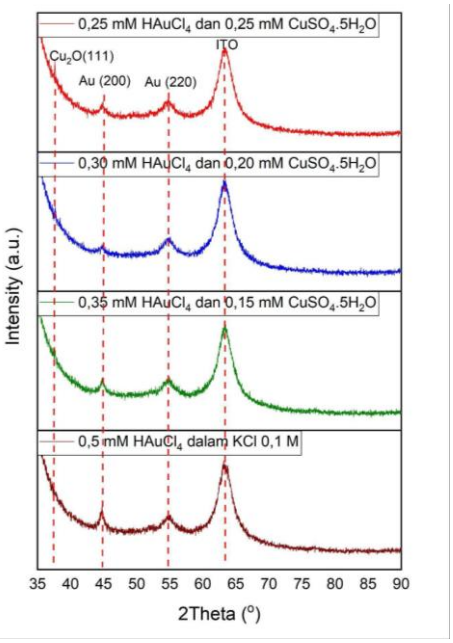

Figure 7. XRD patterns on ITO substrate a) Au-1 (red); b) AuCu-2 (blue); c) AuCu-3 (green); and d) AuCu-4 (brown) nanoparticles.

The XRD patterns show a sharp peak around 63-64°, which can be attributed to the ITO substrate, as also reported by Kumar *et al*. (2019) [9]. This peak is not related to the reaction products, but appears as a fixed background signal in all samples. Overall, the XRD results indicate that the molar ratio of Au^{3+}/Cu^{2+} precursors in the electrolyte solution influences the relative intensity of the diffraction peaks and the phase purity of the deposited films

3.4 Antioxidant activity test

Antioxidant activity was evaluated in vitro by the free radical scavenging method using 2,2 diphenyl-1-picrylhydrazyl (DPPH) [35]. The DPPH molecule is a stable free radical and is commonly used to evaluate the antioxidant activity of some compounds or extracts of natural materials [36].

The DPPH assay results (Fig 8) show that the Cu concentration in the AuCu system affects the antioxidant activity, expressed as percent inhibition. The sample without Cu addition (sample Au-1) showed the highest scavenging activity both at 30 min (6.59%) and 48 h incubation (89.09%). In contrast, the addition of Cu to sample AuCu-3 and AuCu-4 (0.25 mM) caused a significant decrease in the inhibition activity within 30 minutes to 0.34% and 1.89%, respectively. The decrease may be due to the less effective formation of active sites on the CuNPs surfaces within a short incubation time, which is not enough to allow optimal electron transfer to DPPH free radicals [37]. The assay also demonstrated that incubation time strongly influenced the inhibition percentage. At 30 min, all samples exhibited low activity, but inhibition increased sharply after 48 h. Pure AuNPs (sample Au-1) showed the highest value (~89%), while the AuCu bimetallic samples ranged from 80-84%. This indicates that the incorporation of Cu did not directly enhance antioxidant activity under these conditions, although it contributed to improved particle homogeneity.

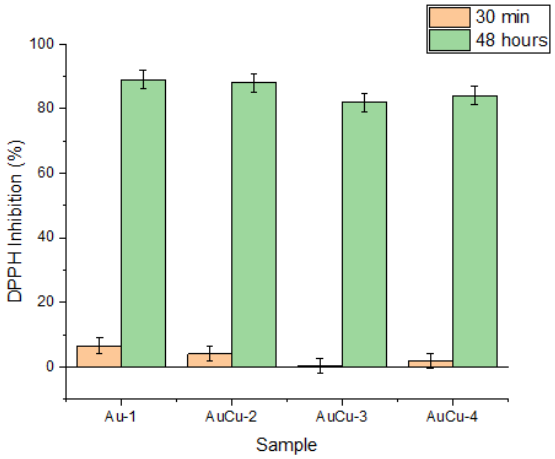

Figure 8. DPPH radical inhibition (%) of Au and AuCu nanoparticles after 30 min and 48 h incubation. Data are expressed as mean ± SD (n=3).

After 48 h of incubation, inhibition values for AuCu-3 and AuCu-4 increased to 82.05% and 84.12%, respectively, though still lower than Au-1. A longer contact time appears to increase Cu's role in radical scavenging, which aligns with its known redox behavior and interaction with π-electron group DPPH [38]. These findings agree with previous reports. Dobrucka showed that biosynthesized CuNPs are more effective scavengers at higher concentrations [34], and Maulina *et al*. (2024) similarly found that CuNPs from *Polyalthia longifolia* extract achieved 68.37% inhibition, with performance improving as concentration increased [39].

The absence of a strong synergistic effect between Au and Cu can be attributed to surface segregation, where Au atoms preferentially occupy the NP surface due to their lower surface energy, thus limiting the exposure of Cu

active sites [40]. Furthermore, the slower electron transfer kinetics of Cu compared to Au make its contribution more apparent only after longer incubation periods. This is consistent with the observed increase in inhibition of AuCu samples at 48 h compared to 30 min. Previous studies have also highlighted that the synergistic effect of AuCu strongly depends on precursor ratio, surface oxidation state, and reaction duration, and that under certain conditions, pure AuNPs can exhibit higher reactivity than the bimetallic form [41]. These results suggest that while AuCu NPs exhibit strong antioxidant activity, the contribution of Cu is time-dependent, and a synergistic effect becomes more evident only at extended incubation times.

The antioxidant activity results showed that pure AuNPs exhibited the highest inhibition value (89.09% after 48 h), which was slightly higher than the AuCu bimetallic samples (82-84%). This finding indicates that the expected synergistic effect between Au and Cu did not appear strongly under the tested conditions. A plausible explanation is related to the phenomenon of *surface segregation*, where Au atoms tend to dominate the nanoparticle surface due to their lower surface energy compared to Cu, thereby limiting the exposure of Cu active sites during the short reaction period [40].

In addition, the electron transfer kinetics of Cu are generally slower than those of Au, so its contribution requires a longer incubation time to become evident. This is consistent with the observed increase in inhibition values of AuCu samples after 48 h compared to 30 min incubation, suggesting that Cu plays a time-dependent role in the radical scavenging process. Previous studies have also reported that the synergistic effect of AuCu NPs is highly dependent on precursor ratio, surface oxidation state, and reaction duration, and that under certain conditions Au alone can exhibit higher immediate reactivity than the bimetallic form [41]. Therefore, the results of this study suggest that although AuCu NPs display good antioxidant activity, their synergistic contribution is more pronounced at longer contact times rather than in the initial phase of the reaction.

3.5 Proposed radical scavenging mechanism

The proposed mechanism for free radical suppression by AuCu NPs is illustrated in Fig 9. The mechanism suggests that the Au atoms on AuCu NPs stabilize the nitrogen (N) atom in DPPH by forming a bond. This is because free radical compounds are very reactive and always try to find electron pairs to stabilize their condition [42]. The N atom donate its lone electron pair to the Au atom, forming a coordination covalent bond that stabilizes the free radicals [43].

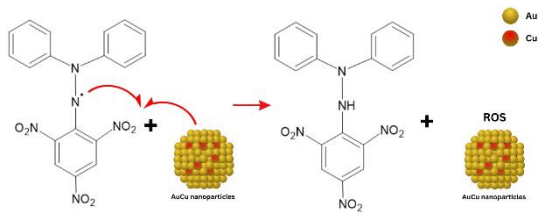

Figure 9. Free radical scavenging proposed mechanism by AuCu nanoparticles.

3.6 MTT assay

MTT assay was performed indirectly to evaluate the cytotoxic and cytoprotective effects of AuCu NPs on HaCaT cells. In the cytotoxic assay, cells that were not exposed to blue light were treated with the immersion solution of each sample.

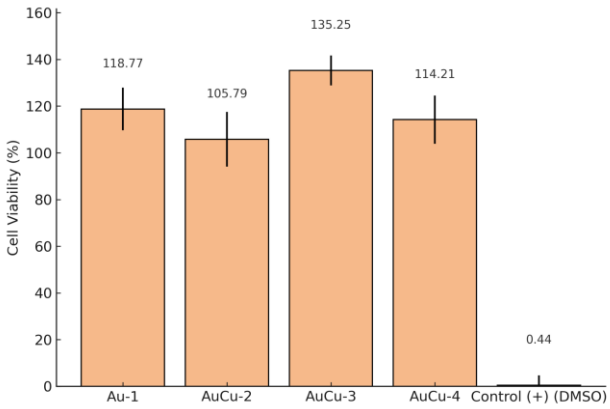

Figure 10. Cytotoxicity assay of AuCu nanoparticles on HaCaT cells. Data are expressed as mean ± SD (n = 3, error bars).

The results in Fig 10 show that all samples had cell viability values above 100%, with the highest value recorded in SIII at 135.25%, indicating that the samples were not only non-toxic, but also able to stimulate cell proliferation. The lowest viability value was found in the positive control, DMSO, at 0.44%, which reinforces the effectiveness of the system as a toxicity reference. This high viability indicates that AuCu NPs do not cause direct cell damage and even have the potential to exert a stimulative effect on cells, especially under conditions without external oxidative stress. This is consistent with the findings of Kwak *et al*. (2022), who reported that AuNPs from green synthesis showed no cytotoxic effect against HaCaT cells at concentrations up to 50 µg/mL [44]. In addition, the study by Philip *et al*. (2024) on green CuNPs synthesized using *Crossandra infundibuliformis* extract showed HaCaT viability >70% even at high concentrations up to 200 µg/mL, indicating minimal toxicity and potential to support cell recovery [45].

In the cytoprotective assay, which involved a 6-hour blue light exposure, all samples maintained HaCaT cell viability at a relatively high level, with the highest viability

value in sample Au-1 at 106.44%, approaching or exceeding the value of cell control (100.08%) and vitamin C positive control (97.73%). These results indicate that the immersion solution of AuCu NPs has the ability to protect cells from oxidative stress damage induced by blue light. This protective effect most likely originates from a free radical scavenging mechanism mediated by the active surface of the bimetallic metal particles. As described by Jomova *et al*. (2024), certain metal NPs, including Cu and Au in oxide or alloy structures, are able to act as nanozymes that mimic the activity of enzymes such as superoxide dismutase (SOD) and catalase, thereby decreasing the accumulation of reactive oxygen species (ROS) in the cellular environment and preventing oxidative damage to skin cells [46]. Therefore, this AuCu NPs system has potential cosmetic and dermatological applications, especially as a protective agent against oxidative stress due to blue light exposure.

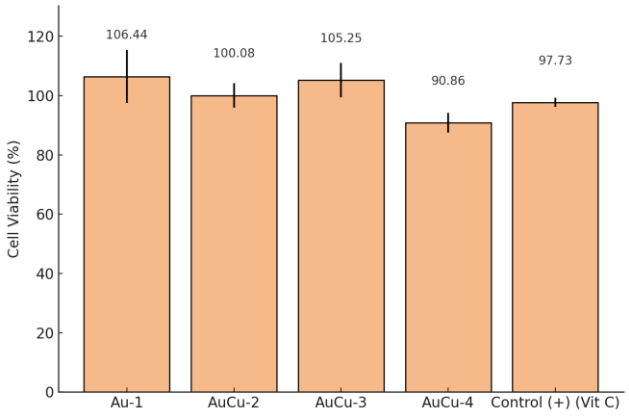

Figure 11. Cytoprotective assay of AuCu nanoparticles on HaCaT cells under blue light exposure. Data are expressed as mean ± SD (n = 3, error bars).

4. Conclusion

Bimetallic AuCu nanoparticles (NPs) were successfully synthesized via electrodeposition method via cyclic voltammetry (CV) with varying concentrations of $CuSO_4$ precursor. The resulting NPs exhibited spherical, dense, and uniformly distributed morphologies on the ITO substrate surface, with average particle sizes ranging from 25 to 57 nm depending on the Au:Cu ratio. Antioxidant activity, evaluated via a DPPH assay, revealed that the pure AuNPs achieved the highest inhibition percentage of 89.09% after 48 hours of incubation. Although the addition of Cu initially reduced the inhibition activity at 30 minutes, it significantly improved over longer incubation, reaching up to 84.12% for a 1:1 Au:Cu ratio. MTT assay results showed that all samples were non-toxic to HaCaT cells and even enhanced cell viability while exhibiting protective effects against blue light-induced oxidative stress. Overall, these findings confirm that the Au:Cu ratio in electrodeposition directly influences NP morphology, size, antioxidant efficacy, and biocompatibility, highlighting AuCu NPs as promising candidates for biomedical and cosmetic nanotechnology applications.

Author contributions

Norma Nurul Ilmi: Investigation, Formal analysis, Writing-original draft. **Putri Dwi Candra**: Investigation, Formal Analysis, Conceptualization. **Sabrina Putri Chaerani:** Visualization, Writing-Review and Editing, Project Administration. **Shirly Harissyah Alfiani:** Methodology, Software, Formal Analysis, Supervision.

Conflicts of interest

The authors declare no conflicts of interest

Acknowledgement

The authors acknowledge that this work was funded by Universitas Negeri Jakarta through the KI research scheme 2025 with contract number 19/KI/LPPM/III/2025.

References

[1] Lobo, V., Patil, A., Phatak, A., & Chandra, N. (2010). Free radicals, antioxidants and functional foods: Impact on human health. *Pharmacognosy Reviews, 4*(8), 118-126. https://doi.org/10.4103/0973-7847.70902

[2] Pham-Huy, L. A., He, H., & Pham-Huy, C. (2008). Free radicals, antioxidants in disease and health. *International Journal of Biomedical Science, 4*(2), 89-96. https://www.ncbi.nlm.nih.gov/pmc/articles/PMC3614697/

[3] Uttara, B., Singh, A. V., Zamboni, P., & Mahajan, R. T. (2009). Oxidative stress and neurodegenerative diseases: A review of upstream and downstream antioxidant therapeutic options. *Current Neuropharmacology, 7*(1), 65-74. https://doi.org/10.2174/157015909787602823

[4] Valko, M., Leibfritz, D., Moncol, J., Cronin, M. T. D., Mazur, M., & Telser, J. (2007). Free radicals and antioxidants in normal physiological functions and human disease. *The International Journal of Biochemistry & Cell Biology, 39*(1), 44-84. https://doi.org/10.1016/j.biocel.2006.07.001

[5] Birben, E., Sahiner, U. M., Sackesen, C., Erzurum, S., & Kalayci, O. (2012). Oxidative stress and antioxidant defense. *World Allergy Organization Journal, 5*(1), 9-19. https://doi.org/10.1097/WOX.0b013e3182439613

[6] Prior, R. L., Wu, X., & Schaich, K. (2005). Standardized methods for the determination of antioxidant capacity and phenolics in foods and dietary supplements. *Journal of Agricultural and Food Chemistry, 53*(10), 4290-4302. https://doi.org/10.1021/jf0502698

[7] Wang, Y., Yang, Y., Shi, Y., Song, H., & Yu, C. (2018). Antibiotic-free antibacterial strategies enabled by nanomaterials: Progress and perspectives. *Advanced Materials, 30*(1), 1704842. https://doi.org/10.1002/adma.201904106

[8] Iravani, S. (2011). Green synthesis of metal nanoparticles using plants. *Green Chemistry, 13*(10), 2638-2650. https://doi.org/10.1039/C1GC15386B

[9] Kumar, K., Kumar, R., Jasrotia, R., *et al*. (2024). In-vitro bactericidal and anti-oxidant efficacy of biosynthesized CuO/Cu_2O-NiO nanocomposites against pathogenic bacteria and DPPH free radical. *Discovery Applied Sciences, 6*, 87. https://doi.org/10.1007/s42452-024-05679-7

[10] Ge, X., Cao, Z., & Chu, L. (2022). The antioxidant effect of the metal and metal-oxide nanoparticles. *Antioxidants, 11*(4), 791. https://doi.org/10.3390/antiox11040791

[11] Dykman, L., & Khlebtsov, N. (2012). Gold nanoparticles in biomedical applications: Recent advances and perspectives. *Chemical Society Reviews, 41*(6), 2256-2282. https://doi.org/10.1039/C1CS15166E

[12] Liu, H., Li, Y., Sun, S., Xin, Q., Liu, S., Mu, X., ... Zhang, X.-D. (2020). Catalytically potent and selective clusterzymes for modulation of neuroinflammation through single-atom substitutions: Au_4Cu_1 clusterzyme exhibits superior catalase-like activity. *arXiv*. https://arxiv.org/abs/2012.09527

[13] Negahdary M., Chelongar R., Zadeh S.K., Ajdary M. (2015). The antioxidant effects of silver, gold, and zinc oxide nanoparticles on male mice in in vivo condition. *Adv Biomed Res*. 4:69. doi: 10.4103/2277-9175.153893

[14] Kus-Liśkiewicz M., Fickers P., Ben Tahar I. (2021). Biocompatibility and Cytotoxicity of Gold Nanoparticles: Recent Advances in Methodologies and Regulations. *Int J Mol Sci.* 22(20): 10952. doi: 10.3390/ijms222010952.

[15] Seyedeh Masoumeh Ghoreishi, Sobhan Mortazavi-Derazkola. (2025). Eco-friendly synthesis of gold nanoparticles via tangerine peel extract: Unveiling their multifaceted biological and catalytic potentials. *Heliyon.* Volume 11, Issue 1. https://doi.org/10.1016/j.heliyon.2024.e40104

[16] Tahir, K. *et al.* (2015). Nerium oleander leaf extract mediated synthesis of gold nanoparticles and their biological applications. *Arabian Journal of Chemistry*, 8(6), 860–871.

[17] Vo, T. T. T., Peng, T.-Y., Nguyen, T. H., Bui, T. N. H., Wang, C.-S., Lee, W.-J., Chen, Y.-L., Wu, Y.-C., & Lee, I.-T. (2024). The crosstalk between copper-induced oxidative stress and cuproptosis: A novel potential anticancer paradigm. *Cell Communication and Signaling, 22*(1), 353. https://doi.org/10.1186/s12964-024-01726-3

[18] Mehdizadeh, T., Zamani, A., & Abtahi Froushani, S. M. (2020). Preparation of Cu nanoparticles fixed on cellulosic walnut shell material and investigation of its antibacterial, antioxidant and anticancer effects. *Heliyon, 6*(3), e03528. https://doi.org/10.1016/j.heliyon.2020.e03528

[19] Laxmi Sonawane, Ram Sonawane, Abhinay Mandawade, Sana Khan, Ganesh Kande, Lalita Jondhale, Pratibha Loke. (2021). Green Synthesis of Copper Nanoparticles Mediated By Dioscorea Bulbifera Tuber for Biofilm Inhibition. *International Journal of Scientific Research in Science and Technology (IJSRST)*, 9(2), 66-71. ISSN: 2395-6011.

[20] Rajeshkumar, S., Menon, S., Venkat Kumar, S., Tambuwala, M. M., Bakshi, H. A., Mehta, M., Satija, S., Gupta, G., Chellappan, D. K., Thangavelu, L., & Dua, K. (2019). Antibacterial and antioxidant potential of biosynthesized copper nanoparticles mediated through *Cissus arnotiana* plant extract. *Journal of Photochemistry and Photobiology B: Biology, 197*, 111531. https://doi.org/10.1016/j.jphotobiol.2019.111531

[21] Bracey, C. L., Ellis, P. R., & Hutchings, G. J. (2009). Application of copper-gold alloys in catalysis: Current status and future perspectives. *Chemical Society Reviews, 38*(8), 2231-2243. https://doi.org/10.1039/b817729p

[22] Elabbadi, M., Boukouvala, C., Hopper, E. R., Asselin, J., & Ringe, E. (2023). Synthesis of controllable Cu shells on Au nanoparticles by electrodeposition: A systematic in situ single particle study. *The Journal of Physical Chemistry C, 127*(10), 5044-5053. https://doi.org/10.1021/acs.jpcc.2c08910

[23] Van Thuan, D., Khoa, N. T., Kim, S. W., Kim, E. J., & Hahn, S. H. (2015). Morphology-dependent selective hydrogenation catalysis of hollow AuCu bimetallic nanostructures. *Journal of Catalysis, 329*, 144-150. https://doi.org/10.1016/j.jcat.2015.05.001

[24] Blosi, M., Ortelli, S., Costa, A. L., Dondi, M., Lolli, A., Andreoli, S., Benito, P., & Albonetti, S. (2016). Bimetallic nanoparticles as efficient catalysts: Facile and green microwave synthesis. *Materials (Basel), 9*(7), 550. https://doi.org/10.3390/ma9070550

[25] Razzaq, H., Saira, F., Yaqub, A., Qureshi, R., Mumtaz,

M., & Saleemi, S. (2016). Interaction of gold nanoparticles with free radicals and their role in enhancing the scavenging activity of ascorbic acid. *Journal of Photochemistry and Photobiology B Biology*, *161*, 266-272. https://doi.org/10.1016/j.jphotobiol.2016.04.003

[26] Suliasih, B. A., Kurniawan, D. G., Auliya, A., & Angelina, M. (2023). Scan rate dependent factor for antioxidant activity of gold nanofilms synthesized via cyclic voltammetry technique. *Chemistry and Materials,* *2*(2), 51-55. https://doi.org/10.56425/cma.v2i2.60

[27] M. Yashini, S. Shanmugasundaram. (2023). Optimization of parameters influencing the electro-deposition of Gold nanoparticles on electrode using Taguchi method. *Pharma Innov.* J.10(2021) 2023-2030. http://www.thepharmajournal.com .

[28] Tang, X., Hu, Z., Wang, Z., Chen, J., Mu, X., Song, G., Sun, P., Wen, Z., Hao, J., Cong, S., & Zhao, Z. (2022). ITO/Cu multilayer electrodes for high-brightness electrochromic displays. *EScience, 2*(6), 632-638. https://doi.org/10.1016/j.esci.2022.08.005

[29] Senthilkumar, M., Mathiyarasu, J., Joseph, J., Phani, K. L. N., & Yegnaraman, V. (2008). Electrochemical instability of indium tin oxide (ITO) glass in acidic pH range during cathodic polarization. *Materials Chemistry and Physics, 108*(2-3), 403-407. https://doi.org/10.1016/j.matchemphys.2007.10.030

[30] Zhang, X., Lou, B., Li, D., Hong, W., Yu, Y., Li, J., & Wang, E. (2015). A universal method for the preparation of functional ITO electrodes with ultrahigh stability. *Chemical Communications, 51*(31), 6788-6791. https://doi.org/10.1039/C5CC00906E

[31] Suliasih, B. A., & Farhanah, A. (2025). Morphology-dependent antioxidant activity of gold nanoparticles prepared using different electrolyte concentrations. *Journal Name,* *4*(1), 9-15. https://doi.org/10.56425/cma.v4i1.93

[32] Dehghani, F., Mosleh-Shirazi, S., Shafiee, M., Kasaee, S. R., & Amani, A. M. (2023). Antiviral and antioxidant properties of green synthesized gold nanoparticles using *Glaucium flavum* leaf extract. *Applied Nanoscience,* *13*(6), 4395-4405. https://doi.org/10.1007/s13204-022-02705-1

[33] Tejaswini P. Patil, Anuja A. Vibhute, Snehal L. Patil, Tukaram D. Dongale, Arpita P. Tiwari. (2023). Green synthesis of gold nanoparticles via Capsicum annum fruit extract: Characterization, antiangiogenic, antioxidant and anti-inflammatory activities. *Applied Surface Science Advances*, Volume 13, 100372, ISSN 2666-5239, https://doi.org/10.1016/j.apsadv.2023.100372 .

[34] Akilandaeaswari, B., & Muthu, K. (2021). One-pot green synthesis of Au-Ag bimetallic nanoparticles from *Lawsonia inermis* seed extract and its catalytic reduction of environmentally polluted methyl orange and 4-nitrophenol. *Journal of the Taiwan Institute of Chemical Engineers,* *127*, 292-301. https://doi.org/10.1016/j.jtice.2021.07.019

[35] Wulansari, A. N. (2018). Alternative to Purple Cantigi (*Vaccinium varingiaefolium*) as a natural antioxidant: A review. *Farmaka,* *16*(2), 419-429. https://doi.org/10.24198/jf.v16i2.17574

[36] Cahyono, B., Prihatini, C. S., Suzery, M., & Bima, D. N. (2021). Determination of antioxidant activity of quercetin compounds and galangal extract using HPLC and UV-Vis. *Alchemy,* *8*(2), 24-32. https://doi.org/10.18860/al.v8i2.10594

[37] Mehrab Pourmadadi, Roghaieh Holghoomi, Amin shamsabadipour, Reza Maleki-baladi, Abbas Rahdar, Sadanand Pandey. (2024). Copper nanoparticles from chemical, physical, and green synthesis to medicinal application: A review. *Plant Nano Biology,* Volume 8, 2024, 100070, ISSN 2773-1111, https://doi.org/10.1016/j.plana.2024.100070 .

[38] Dobrucka R, Długaszewska J. Biosynthesis and antibacterial activity of ZnO nanoparticles using Trifolium pratense flower extract. Saudi J Biol Sci. 2016 Jul;23(4):517-23. doi: 10.1016/j.sjbs.2015.05.016. Epub 2015 May 31. PMID: 27298586; PMCID: PMC4890195.

[39] Maulana I, Ginting B, Mustafa I, Islami RAN. Green Synthesis of Copper Nanoparticles Using *Polyalthia longifolia* Roots and their Bioactivities Against *Escherichia coli, Staphylococcus aureus*, and *Candida albicans*. J Pharm Bioallied Sci. Jul 2024;16(Suppl 3):S2218-S2223. doi: 10.4103/jpbs.jpbs_1219_23. Epub 2024 May 13. PMID: 39346455; PMCID: PMC11426711.

[40] Breyton, R., Salazar, M., Rosenthal, A., *et al*. (2023). Atomic-Scale Surface Segregation in Copper–Gold Nanoparticles. Physical Review Letters, 130(23), 236201. https://doi.org/10.1103/PhysRevLett.130.236201

[41] Shang H., Kim D., Wallentine S.K., Kim M., Hofmann D.M., Dasgupta R., Murphy C.J., Asthagiri A., Baker L.R. (2021). Ensemble effects in Cu/Au ultrasmall nanoparticles control the branching point for C1 selectivity during CO2 electroreduction. *Chem Sci*, 12(26): 9146-9152. https://doi.org/10.1039/D1SC02602J

[42] Pertiwi, R. D., Utami, T. P., & Michelle, D. (2024). Biosynthesis and antioxidant assay of gold nanoparticles using quercetin. *Archives Pharmacia, 6*.

[43] Musfiroh, E., & Syarief, S. H. (2012). Free radical

scavenging of activity test of gold nanoparticles with various concentrations as antiaging material in cosmetics. *UNESA Journal of Chemistry, 1*(2), 18-25. https://doi.org/10.26740/ujc.v1n2.p%25p

[44] Kwak, G.-Y., Han, Y., Baik, S., Kong, B.-M., Yang, D.-C., Kang, S.-C., & Sukweenadhi, J. (2022). Gold nanoparticles green-synthesized by the *Suaeda japonica* leaf extract and screening of anti-inflammatory activities on RAW 267.4 macrophages. *Coatings, 12*(4), 460. https://doi.org/10.3390/coatings12040460

[45] Philip, R. R., Seetharaman, J., Priya, R. A., Vedakumari, S. W., & Sankari, D. (2024). Biogenic synthesis and characterization of copper nanoparticles using *Crossandra infundibuliformis* leaves and evaluation of antimicrobial, antioxidant, cytotoxic analysis and wound healing activity on HaCaT cell line. *3 Biotech, 14*, 194. https://doi.org/10.1007/s13205-025-04360-z

[46] Jomova, K., Alomar, S. Y., Alwasel, S. H., Nepovimova, E., Kuca, K., & Valko, M. (2024). Several lines of antioxidant defense against oxidative stress: Antioxidant enzymes, nanomaterials with multiple enzyme-mimicking activities, and low-molecular-weight antioxidants. *Archives of Toxicology, 98*(5), 1323-1367. https://doi.org/10.1007/s00204-024-03696-4